JOURNAL OF MULTIFUNCTIONAL MATERIALS & PHOTOSCIENCE
11(2), December 2020, pp. 213-231

Synthesizing of novel photocatalyst and recent advancement in photocatalytic hydrogen evolution

Md Nazmodduha Rafat[1], Is Fatimah[2], Saksit Chanthai[3] and Won-Chun Oh[*]

[1]*Department of Advanced Materials Science & Engineering, Hanseo University, Seosan-si, Chungnam, Korea, 356-706*
[2]*Chemistry Department, Universitas Islam Indonesia, Kampus Terpadu UII, Sleman, Yogyakarta, Indonesia*
[3]*Materials Chemistry Research Center, Department of Chemistry and Center of Excellence for Innovation in Chemistry, Faculty of Science, Khon Kaen University, Khon Kaen 40002, Thaila*

Abstract: The increasing demand for energy is a serious issue worldwide that has attracted the attention of researchers. A large amount of energy is produced from fossil fuels, which have negative effects on the environment and cause pollution. Several different methods and technologies have been introduced to solve the world's energy problems. Photocatalytic water splitting to produce hydrogen is one of the most promising methods with potential to solve the environmental and sustainable energy issues caused by the mass consumption of fossil fuels. It is a cost-effective and ecofriendly method. Over the last few decades, many efforts have been made to design efficient photocatalytic water splitting systems for the production of hydrogen. In this chapter, we examine many water splitting methods, with a focus on photocatalytic water splitting. We also discuss the various materials used as photocatalysts for water splitting. Finally, we review strategies for improving the conditions of hydrogen production. Photocatalytic water splitting at elevated temperatures is emphasized as a novel approach to suppress photo-excitons recombination on catalyst surface owing to adsorption of enhanced concentration of ionic species including H^+ and OH^- to create their local polarization to the excitons. Stronger polarization to hinder the excitons recombination can also be obtained by using polar-faceted support materials to the active phase of semiconductor. It is clearly demonstrated in this minireview that such high temperature promoted photocatalytic water splitting systems could open a new direction and provide an innovation to this field.

1. Introduction

Natural resources such as coal and petroleum products as a source of energy are nearly exhausted [1]. The reduction of fossil fuel reserves has prompted substantial research efforts toward the usage of hydrogen (H_2) as an environmentally friendly energy carrier for the post fossil fuel regime [2]. It is currently generally agreed that H_2 may be the best option for tackling the triple issues of exhaustion, pollution and climate change effects [3]. One of the technologies for H_2 production is photocatalytic water splitting, since it entails photonic energy, which is the most abundant energy resource on the Earth [4].

Previous research states that solar based H_2 generation by photocatalysis provides near zero global warming and air pollutants [5] and can be stored easily [6]. Therefore, H_2 is considered as a possible important energy in future, since it is free from toxic and it can produce high energy content from natural resources such as light (photon) energy and water, which are clean, long lasting sources of energy, and renewable resources [7]. Pioneer work as early as 1972 by Fujishima and Honda [8] reported water splitting for H2 production over TiO2 semiconductor. Since then, various types of semiconductors for photocatalytic H2 productions are under investigation. Among all, titanium dioxide (TiO_2) with band gap 3.2 eV is a recognized photocatalyst and it has been extensively studied because of numerous advantages such as low cost, high photochemical stability and non-toxic [6,9]. On the other hand, wide band gap limits its applications under visible light and faster charges recombination rate lowers its photocatalytic activity [6,10]. Coupling TiO_2 with visible light semiconductors can narrowing the band gap with faster charges separation, thus could enables enhanced photo-catalytic activity. Among the low band gap semiconductors, polymeric graphitic carbon nitride (g-C_3N_4) has attracted more attentions as metal-free polymeric semiconductor in photocatalytic water splitting. It is a visible light responsive with lower band gap and low-cost semiconductor. It can be synthesized from cheap precursors such as melamine and urea by simple thermal approach. In addition, g-C_3N_4 has numerous advantages such as high thermal and chemical stability and appropriate band structure (2.7 eV) to absorb visible light irradiation [11]. Among the limitations, g-C_3N_4 has low surface area and small active sites for interfacial (photon) reaction, moderate oxidation reaction of water to H^+ and low charge mobility which disrupt the delocalization of electrons. Hence, the coupling or/and doping g-C_3N_4 with other elements can overcome its limitations. Among the other alternatives, coupling g-C_3N_4 with TiO_2 to develop type II heterojunction could be promising to get enhanced H_2 production during photocatalytic water splitting under visible light irradiations.

Recently, the formation of Z-scheme photocatalytic system, analogous to artificial photosynthesis, is one of the latest strategies to improve photocatalytic performance as compared to using single semiconductor photocatalyst. Commonly investigated Z-scheme systems have three classifications that are with shuttle redox mediators, without electron mediators, and with solid-state electron mediators [12]. These systems can enhance the efficiency of photocatalyst performance, since it effectively increases the visible light absorption, accelerates the separation and transportation of charge carriers. In addition, surface modification such as catalyst structure and morphology can improve performance due to increasing surface area and efficient charge carrier's separation [13]. The configuration of semiconductors has been designed and investigated in the form of nanoparticles, nanosheets, nanotubes and nanowires [14]. Therefore, semiconductor photocatalyst selection and modification have great potential to narrow the band gap, utilizing visible light and promoting charge separation towards selective H_2 evolution.

The efficiency of water splitting is determined by the band gap and band structure of the semiconductor and the electron transfer process, as shown in Fig. 1. Generally,

for efficient H2 production using a visible-light-driven semiconductor, the band gap should be less than 3.0 eV (420 nm), but larger than 1.23 eV, corresponding to the water splitting potential and a wavelength of ca. 1000 nm. Moreover, the conduction band (CB) and valence band (VB) levels should satisfy the energy requirements set by the reduction and oxidation potentials for H_2O, respectively. Band engineering is thus necessary for the design of semiconductors with these combined properties. The mechanism of photocatalytic water splitting for H_2 production is illustrated as in Fig. 2 [15]. The photo catalysis has four major processes, which are light harvesting (stage 1), charge excitation (stage 2), charge separation and transfer (stage 3 and 4), and surface catalytic reactions (stage 5 and 6) [16]. First, photocatalysis starts with light irradiation with energy greater or equal to the band gap of photocatalyst. Typically, the semiconductor of photo catalyst consists of a VB and a CB, which are separated from one another by a band gap energy (E_g) [17]. The photo-catalyst under appropriate photon excitation causes electronic transitions and generates e^-/h^+ pairs (Eq. (1)). Second, the charges are separated, and the electrons are excited from the VB to CB, leaving holes in the VB. Electrons and holes are involved in the reduction (stage 6) and oxidation (stage 5) reaction with water. The oxidation reaction involves decomposition of water into H^+ as shown in Eq. (3), while Eq. (4) shows reduction reaction when H^+ gains electron to produce H_2. Redox reaction on the surface of photocatalyst occurs when the reduction and oxidation potentials are above and below than CB and VB levels, respectively [26,28-30]. Photo-excited holes are powerful oxidants, capable of oxidizing water and organics such as alcohols as shown in Eqs. (3) and (5), respectively. The reaction can be carried out with thermal dissociation of water at temperature more than 2070 K; however, water splitting can be conducted at room temperature using photocatalyst under light irradiation with energy more than the band gap energy [2].

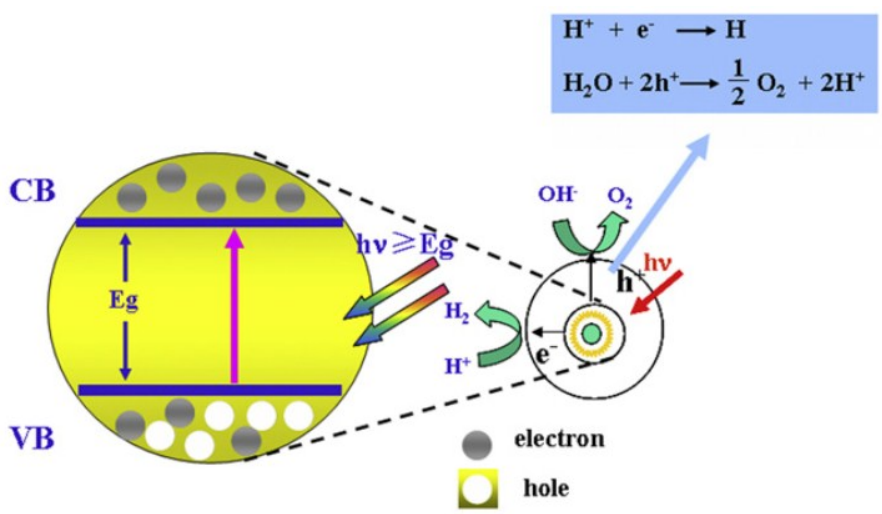

Fig. 1. Fundamental steps during photocatalytic water splitting.[14]

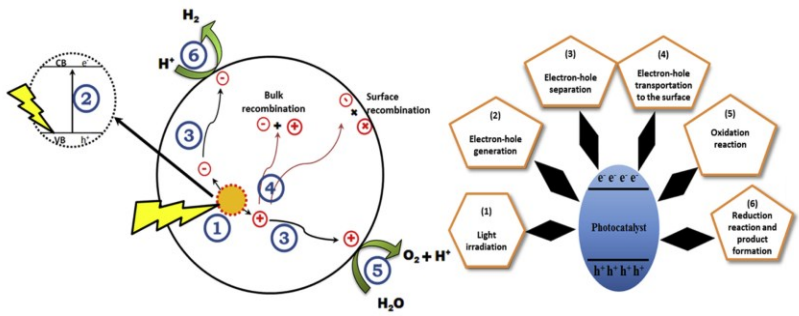

Fig. 2. Illustration of mechanism of photocatalytic water splitting for H_2 production.[15]

Catalyst $\rightarrow$ Catalyst ($e^- + h^+$) (1)

Catalyst ($e^- + h^+$) '! Catalyst (2)

$H_2O + H+ \rightarrow$ ½ $O_2 + 2H^+$ (3)

$2e^- + 2H^+ \rightarrow H_2$ (4)

RCH_2OH +2H '! RCHO + $2H^+$ (5)

However, the major challenge regarding photocatalytic water splitting is the charges (e^-/h^+) recombination. The electron hole pairs could recombine (stage 4) as illustrated in Eq. (2) with the release of unproductive heat. Therefore, it reduces the effectiveness for the H2 generation. Particularly in pure water, it is difficult to achieve water splitting for H_2 production using photo-catalysts due to fast recombination of photo-generated charge carriers. Consequently, photocatalytic water splitting is usually studied in the presence of sacrificial reagent (methanol, ethanol, and glycerol) and electrolytes (Na_2S and KI). The electrolytes are not undergoing reduction or oxidation by CB electrons and VB holes. Electrolytes act as transport of ions and transfer of electrons to adjacent semiconductor. Therefore, they will give improvement on the photocatalytic water splitting reactions. The sacrificial reagent or electron donors are reacting with VB holes to enhance charges separation [18]. Since, the formation of H_2 from pure water has its limitation, the understanding of thermodynamic analysis in terms of energy, band gap and redox potential can enhance the maximum performance for photocatalytic activity.

One of our research, ultrasound wave also has been used to synthesis new material. BaCuZnS -G-TiO_2 has been synthesized through ultrasonic process to minimize the bandgap. The important point is to control the growth and agglomeration time, which differs according to the reductant delivery rate, reductant concentration, and ultrasonic power [10-23]. An ultrasonic wave is defined as the frequency of sound beyond the range of human hearing, typically at 16 kHz. Above this range, more acoustic energy can be conveyed by the sound waves. This energy is transferred to the reaction through the generation of heat and pressure [24-25]. Ultrasound is commonly used for materials testing and medical diagnosis, and its application can be divided into two parts: low

intensity and high intensity. The ultrasonic intensity can also be described as the power density of the acoustic wave (W) applied to a unit area of the medium (square centimeters) [26, 27]. Low-intensity ultrasound is used for material testing and diagnosis by transmitting non-destructive levels of energy through a medium in order to get information [27]. Chemical applications of ultrasound are 20 – 100 kHz. The low intensity of power carried by the acoustic wave has a very restricted influence on the applied medium and does not affect chemical reactivity [28, 29].

In the preparation of this quaternary material, we used Ba, Cu, and Zn because of their super-conductive properties and good affinity with sulfur and other materials. Other studies [30, 31] show that ZnS and CdS nanoparticles are efficient as a visible active material. However, our study goal is to minimize the band gap and make small size material. Because ZnS contains 3.6 eV of band-gap energy, our introduced quaternary material has a narrow band gap, between 3.15-3.26 eV. Our selected precursor materials, Ba, Cu, and Zn have excellent conductive properties and sulfur has good affinity and semiconducting properties. As a quaternary material, BaCuZnS has shown a good photocatalytic effect in the photocatalytic experiment for hydrogen evolution via water splitting under visible light. Moreover, the addition of graphene and TiO_2 also helps to tailor the band-gap energy [32]. Titanium dioxide has taken a place as a relievable photocatalyst in the last few decades because of its low cost, nontoxicity, high photochemical stability, and suitable electronic properties [33]. Because of the small band gap, the catalytic performance of TiO_2 under visible light is promising [34]. Furthermore, the implementation of ultrasound waves increases the hydrogen evolution amount. The ultrasound wave has a high frequency, which increase the manifold in a variety of chemical reactions. Because of the ultrasound effect, the average distance between the molecules increases [35]. When the average distance between the molecules exceeds the critical molecular distance necessary to hold the liquid intact, the liquid breaks down; cavities (cavitation)' and bubbles are formed. These bubbles can be filled with gas or vapor and occur in water, organic solvents, biological fluids, molten metals, or other fluids [36, 37].

To split water using solar energy, semiconductor photocatalysts, such as TiO_2, $SrTiO_3$, Nb_2O_5, SiC, CdS and GaP [38], etc. have obtained much attention. Various modification methods such as doping [39], sensitization, and hybrid composite etc have been attempted. Up to now, over 130 materials and derivatives have been developed to photocatalyzed the overall water splitting or produce hydrogen/ oxygen in the presence of external redox agents. Combinatorial method has been developed that has been demonstrated as a convenient way for quick selection of photocatalyst materials [40–42]. It is considered that the low efficiency for the hydrogen production of semiconductor already with appropriate band gap is due to the following reasons: 1) quick electron/hole recombination in the bulk or on the surface of semiconductor particles, 2) quick back reaction of oxygen and hydrogen to form water on the surface of catalyst, and 3) inability to efficiently utilize visible-light. It was often observed that photo-generated electrons easily recombine with holes in the semiconductor. This recombination leads to the low quantum efficiency of photocatalysis

[43]. Noble metal loading can suppress to some extent the charge recombination by forming a Schottky barrier. More often various sacrificial reagents such as inorganic salts and organics were added in the reaction media, effectively restraining the charge recombination process and improve quantum efficiency [44]. Separation of hydrogen gas is also required as oxygen and hydrogen are produced simultaneously. This could be achieved by employing a photoelectron-chemical system, in which hydrogen and oxygen are produced at different electrodes. The most often studied photocatalysts that have suitable band gaps for photocatalytic hydrogen production are illustrated in Fig. 3. Among these materials, Pt-loaded CdS photocatalyst is the earliest and most studied showing high activity for H_2 production from aqueous solutions containing S^{2-} and SO_3^{2-} ions as sacrificial electron donors, under visible-light irradiation.

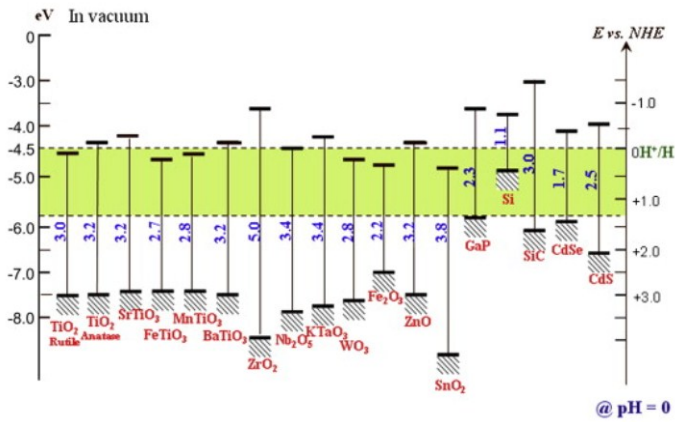

Fig. 3. The band gap positions for various traditional semiconductors relative to the redox potential of water.[44]

2. Experimental Method

There exists interest for the large-scale production of nanostructured materials of bare or doped semiconductor photocatalysts. Numerous reports have been presented regarding the synthesis, characterization, and photocatalytic activity evaluation of undoped and doped (metal or nonmetal) titanium dioxide, for example. It has been demonstrated that the physicochemical properties and photocatalytic activity of semiconductors are mainly determined by the preparation technique used in its production. Photocatalytic semiconductors can be prepared in the form of powders, fibers, and films by different synthetic methods including sol-gel process, hydrothermal and solvothermal techniques, direct oxidation reactions, sonochemical method, microwave method, chemical vapor deposition method, and electrodeposition method, among others. In this section will be briefly reviewed the principles that govern some of the most used synthetic methodologies employed to obtain photocatalytic materials, most of them related to graphene and modified TiO_2.

2.1 Solid solution Photocatalyst

In recent years, solid solution photocatalysts with controlled electronic structures has

been suggested as a promising direction. Various solid solutions such as (GaN)(ZnO) [45], $(AgIn)_xZn_{2(1-x)}S_2$ sulfide solution [46] and other oxide solution [47] have been developed for photocatalytic hydrogen production in pure water, sulfide and alcohol. ZnS with 3.6 eV band gap is a well-known photocatalyst for H_2 evolution though it responds to only UV. It shows high activity without any assistance of co-catalysts such as Pt. Chen et al. reported a nano porous $ZnS–In_2S_3–Ag_2S$ solid solution synthesized by a facile template-free method that showed high activities for H_2 evolution under visible-light irradiation in the absence of co-catalysts. The initial rate of photocatalytic hydrogen yield reached 3.3mmolh^{-1} with 0.015 g photocatalyst employed [48]. In view of practical application of photocatalytic hydrogen production technique, cost reduction of the photocatalyst is one of the key issues. Thus, active photocatalysts free of noble metal like $Cd_{1-x}Zn_xS$ is valuable in this consideration. The controllable band structure of this solid solution further adds its value for industrial application. A series of $Cd_{1-x}Zn_xS$ (x ¼ 0–0.92) photocatalysts were prepared by co-precipitation method and were calcined at 723 K underN2 atmosphere [49]. The band gap of the photocatalyst can be continuously adjusted by changing the composition of the solid solution (see Fig. 4). At the optimal composition, the solid solution showed high activity toward hydrogen production even in the absence of noble metal loading. However, $Cd_{1-x}Zn_xS$ prepared by conventional co-precipitation method often shows poor crystallinity. The activity and stability of the prepared material is far from being satisfactory for its commercial utilization. Recently, in our group a series of $Cd_{1-x}Zn_xS$ solid solution photocatalysts was prepared by thermal sulphuration of corresponding oxide precursors [50]. The band gap control of solid solution photocatalyst can also be achieved by varying its composition. The final composition for all the samples prepared by thermal sulphuration of corresponding mixed precursors is close to their stoichiometric composition. It is found that Cd0.8Zn0.2S solid solution with nominal x value of 0.2 showed the highest activity toward hydrogen production as shown in Fig. 5, the quantum efficiency achieves 9.6% at 420 nm.

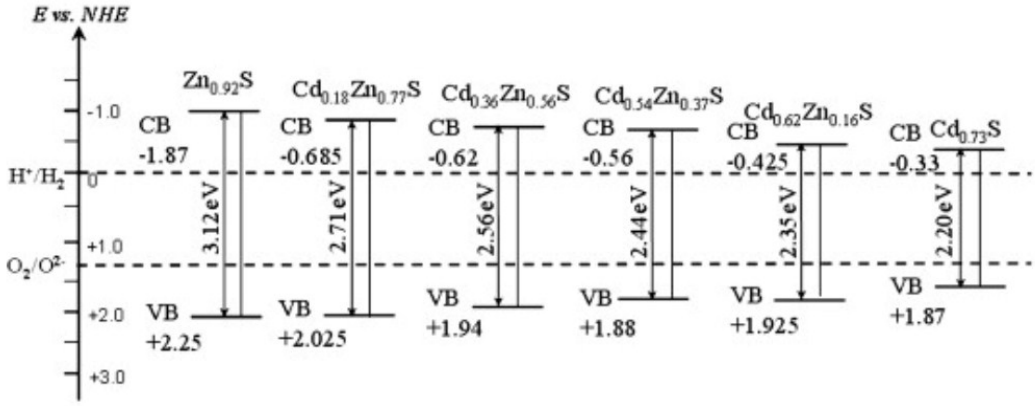

Fig. 4 Conduction and valence band potentials of the $Cd_{1-x}Zn_xS$ photocatalysts with various Cd/Zn ratios.[49]

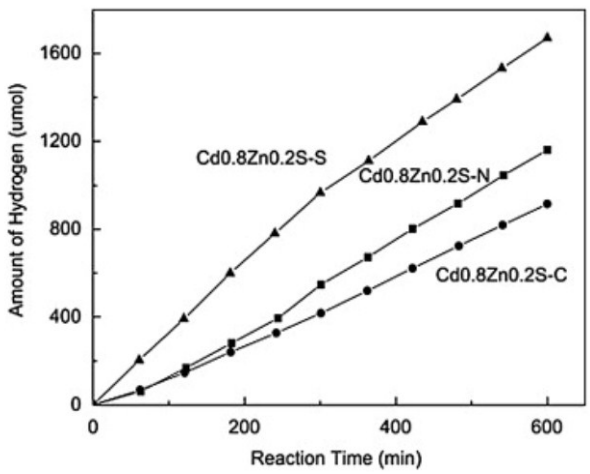

Fig. 5. Hydrogen production for $Cd_{1-x}Zn_xS$ solid solution prepared by various methods. a) $Cd_{0.8}Zn_{0.2}S$–S, prepared by two-step thermal sulfuration (b) $Cd_{0.8}Zn_{0.2}S$–C, prepared by co-precipitation (c) $Cd_{0.8}Zn_{0.2}S$–N, prepared by two thermal sulphuration under N_2 atmosphere.[50]

2.2 *Formation of hybrid or composite photocatalyst*

Coupling of two photocatalyst has been considered effective for improvement of photocatalytic efficiency. To extend the light absorption of such wide band gap semiconductors as TiO_2 and Ta2O5, it is doped with cationic and anionic ions [52– 53]. In our study, nitrogen doped TiO_2 was coupled with WO3 and after loaded with noble metal, high efficiency was obtained [51]. CdS nanocrystallites have been successfully incorporated into the mesopores of Ti-MCM-41 by a two-step method involving ion-exchange and sulphuration forming a CdS@Ti-MCM-41 composite photocatalyst. Owning to the quantum confinement effect and efficient charge separation, the activity of CdS photocatalyst has been greatly improved [54,55]. The activity of CdS@Ti-MCM-41 was much improved by loading Pt co-catalyst. This demonstrates that Ti-MCM-41 serves as a stable host to protect the loaded CdS particles from photo corrosion. In another study, CdS nanoparticles were decorated on $Na_2Ti_2O_4(OH)_2$ nanotubes through partial ion exchange method [56]. The results showed that the high activity of the prepared composite photocatalyst can be attributed to the enhanced charge separation due to the one-dimensional nanotube structure of the $Na2Ti_2O_4(OH)_2$. This further suggests that materials with special morphology or structure are favorable for enhanced photo utilization.

2.3 *Graphene as electron mediator*

Another strategy to suppress the electron-hole pairs recombination is the application of graphene as the electron mediator in the Z-scheme photocatalytic system [58,59, 60]. As an electron mediator, interlayer graphene acts as a bridge and immediately transport the electrons from one semiconductor to another semiconductor as shown in Fig. 6. For

example, Lang et al., [57] reported higher water splitting efficiency of Ag/rGO/TiO_2 composite as rGO acted as electron mediator by providing efficient electron transfer between Ag and TiO2. The photo-generated hot electrons produced by SPR effect in Ag metal were transferred from CB of Ag to VB of TiO_2 through the graphene layer. Efficiency of rGO mediated composites was significantly high compared to simple heterojunction of Ag/TiO_2. Apart from high activity, faster electrons shuttling capability of rGO induce stability to metal catalysts [57]. Similar behavior of graphene was observed in rGO supported Au deposited TiO2 (AuTiO_2/rGO), where graphene served as rapid electron transfer unit.

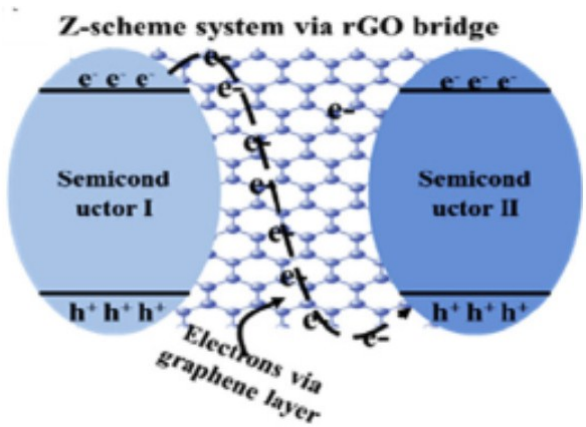

Fig. 6. Graphene as electron mediator in Z-scheme photocatalysts.[57]

2.4 Graphene as p-N type heterojunction

In n-p heterojunction composites, graphene acts as p-type material having holes as majority carrier. As illustrated in Fig. 7, when n-type semiconductor was coupled with ptype graphene, the electrons were transmitted in one direction like in heterojunction and remarkably reduced the electrons-holes recombination [61]. Chen et al. [62] reported p-type GO integrated with n-type TiO_2, where p-n type II heterojunction effectively inhibited the charge carrier recombination and led to higher H2 production. In addition, Lu et al. [63] developed three-dimensional graphene material which was able to inject electrons into conduction bands of TiO_2. Hot electrons generated in graphene were transported to TiO_2 due to higher CB level of graphene than conduction band of TiO_2. This drastically enhanced the electron density in the intermediate's states and the production of H_2. Similarly, surface heterojunction of anatase TiO_2- graphene-rutile TiO_2 exhibited vectorial transfer of charge carriers and resulted in higher production of H2 than rutile and anatase TiO_2 [64]. Moreover, p-type character of graphene can be further reinforced by doping of graphene with trivalent non-metal impurity such as boron (B) that reduce the defect density [65]. For example, Xing et al. [66] reported that when less defective boron doped graphene was coupled with TiO_2, it acted like facilitator in transmitting the electrons from TiO_2 to p-type graphene and inhibited the charge recombination.

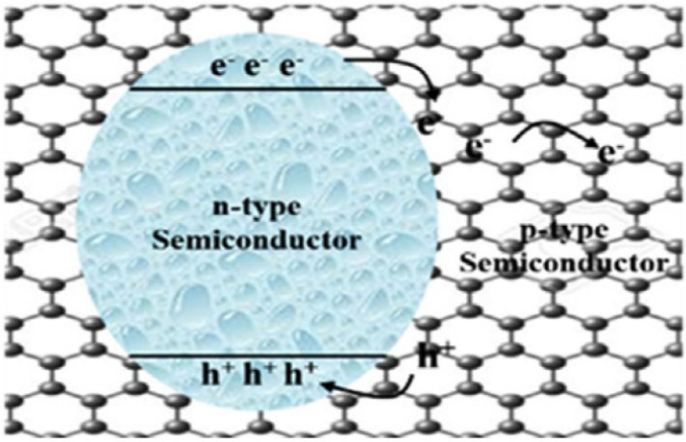

Fig. 7. Graphene as p-type material.[61]

2.5 Graphene as N-N type heterojunction

Now-a-days much attention has been given to doping of N into graphene which constitute n-type semiconductor characteristics. This is due to the its similar atomic size and larger valence electron number of nitrogen atoms as compared to those of carbon atoms [67,68-71]. This makes it advantageous for its application in super capacitors, fuel cells and field-effect transistors and photocatalysis [72]. The n-type N-doped graphene offer a unique 2D sp^2-hybridized carbon network. This also induces improved charge transfer properties as well as increased specific surface area [73]. Mou et al. [74] studied N-GO/ TiO_2 composite by utilizing nitrogen doped graphene. Improved electrical conductivity was showed by NGO as compared to conventional rGO. This was because of effective structural rebuilding as well as lesser defects in structure of GO. Graphene has been employed with different binary semiconductors such as TiO_2, Ag_3PO_4, g-C_3N_4 and Cu_2O to improve dispersion, develop heterojunction, working as mediator, promoting charges separation and improving visible light absorption. However, highest photocatalytic hydrogen production was observed when a metals/non-metal were integrated in a composite of RGO with semiconductor due to boosting charge carrier separation and SPR effects under visible light irradiation.

3. Result and Discussion

Combining TiO_2 with other semiconductors through type I, II and III hetero junctions, constructing Z-scheme and S-type photocatalytic system are important methods to maximize efficiency for photocatalytic hydrogen production under visible light irradiation [75]. The heterojunction of TiO_2 can be constructed using semiconductors with more negative CB values than TiO_2. For example, a type I heterojunction of g- C3N4/Fe_2O_3 with Pt as co-catalyst for enhanced photocatalytic H_2 evolution has been reported [76]. The enhanced photocatalytic activity was observed due to electrons and holes transporting towards Fe_2O_3 surface, resulting in 1150 times high H2 evolution than

using pristine TiO2 due to faster charge carrier separation. In another development, type II heterojunction of NiO-TiO_{2-x}-C composites constructed for enhanced photocatalytic hydrogen production as demonstrated in Fig. 8 (a). Carbon nanosheets improve dispersion of TiO_2, whereas NiO facilitates the separation of charge carrier and enhances the photoactivity under visible light irradiation, which are 18 folds higher than using TiO_2/C [76]. Likewise, $Bi_4Ti_3O_{12}/TiO_2$ composite formed type I heterojunction which enhanced photocatalytic performance because of effective charge carrier transfer and improved visible light utilization. Type I heterojunction promoted the activation of wider band gap TiO_2 under visible light and the H^+ to H_2 reaction took place on surface of $Bi_4Ti_3O_{12}$ [77]. In the development of type II heterojunction, g-C_3N_4/TiO_2 composite is famous, where photo-excited electrons transferred to TiO_2 for oxidation and holes were transferred to g- C_3N_4 monolayer for redox reaction, resulting in inhibited charge carrier recombination. Moreover, extra electrons were provided for H_2 production reaction due to the synergic effect raised by the favorable CB positions of g-C_3N_4 and TiO_2 in heterojunction [78]. As another example, fabricated TiO/ $BiFeO_3$ nanocomposite showed improved H_2 production due to the transfer of electrons generated in BiFeO3 under visible light (l -500 nm) to TiO_2, which promotes photo-generated charge carriers' separation [79]. Umer et al., studied SWCNTs/TiO_2 heterojunction composite for dynamic H_2 generation. TiO_2 was not completely activated under visible-light irradiations leading to recombination, however; montmorillonite (Mt) and SWCNTs were capable of absorbing visible light, leading to TiO_2 activation [80]. Visible light activity was observed for CdS/TiO_2 composite by formation of type II heterojunction in which the low band gap of CdS assisted the transfer of photo-generated excited electrons from CdS nanoparticles to crystalline TiO_2 [81]. Besides, for enhancement of activity by co-dopants, carbon nanotubes (CNTs) are also another alternative of potential hybrid for TiO_2 doping. Carbon could act as an electron sink, which prevents the recombination process. Thus, employing co-catalyst is a promising system to maximize photocatalytic hydrogen production under visible light. In the Z-scheme development, water splitting through photocatalysis was first introduced by Bart et al., [82] in 1979, since then this approach has gained much attention and is considered as an efficient method to enhance photocatalytic hydrogen production. This $CuGaS_2$/rGO/TiO_2 as a Z scheme heterojunction supported by solid state electron meditator was studied for visible light photocatalytic activity. Upon illumination by visible light, the electrons in CB of TiO_2 and holes in VB of CuGaS2 were recombined by the rGO as mediator. Hence, the holes left in VB of TiO_2 and electrons in CB of leaving holes in TiO_2 and electrons in $CuGaS_2$ lead efficient water splitting [83]. Another technique for modification of semiconductors is cooping in which low band gap of one material induces photocatalytic activity in a wide band gap material [84]. Co-doping increases the charge separation and improves the range of photo-excitation energy in the process. For instance, in case of co-doping of TiO_2 and WO_3, the narrower band gap of WO_3 utilizes solar irradiation better than TiO_2, and underwent photoexcitation, creating electrons and holes. The photo-generated electrons were transferred to TiO_2 conduction band, leaving behind holes in WO_3 valence band. This long emigration time of electron transfer increases the charge separation

leading to redox reaction [85,86]. For example, TiO_2 anatase is inactive under visible light because of 3.2 eV band energy, but $BiVO_4/TiO_2$ heterojunction induces visible light activity in TiO_2 and led to efficient charge separation and transfer [87]. Fig. 8 (b) depicts Z-scheme heterojunction system of WO_3/TiO_2 with plasmonic effect of Au for enhanced photocatalytic hydrogen under visible light irradiation. The H_2 evolution rate over Au-WO_3/TiO_2 was increased by 6 folds due to SPR effect of Au and proficient charge carrier separation among the semiconductors [88]. Fig. 8 (c-e) demonstrated core-shell Z-scheme heterojunction of TiO2/NiS hybrid nanofibers with enhanced stability for photocatalytic hydrogen production. The H_2 evolution rate of 14.6-fold higher over composite was achieved than using only pristine TiO_2. This enhanced photocatalytic activity was due to direct Z-scheme heterojunction formation, which greatly promotes the separation of electrons and holes [89]. A recent development in TiO_2 based heterojunction formation with binary semiconductors has been summarized in. Obviously, different types of semiconductors such as NiO, CdS, Ag_2O, Bi_2O_3, RuO_2, ZnO, CoO, ZrO_2, SnO_2 and WO_3 have been employed in the formation of TiO2 heterojunction. According to all above discussion, type II and Z scheme heterojunction formations are effective methods to enhance visible light absorption and promotes charge carrier separation to get higher hydrogen production during photocatalytic water splitting under visible light irradiation. However, Z-scheme heterojunction is more promising due to getting more negative CB and more positive VB during band adjustment of semiconductors, which is favorable to get higher hydrogen production and can be employed in other solar energy applications.

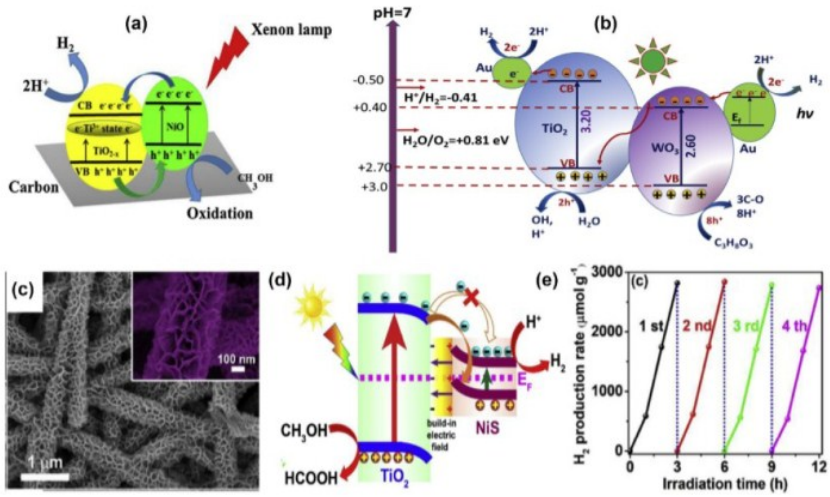

Fig. 8. (a) Schematic illustration of type II heterojunction of NiO/TiO2 for photocatalytic hydrogen production, (b) Direct Z-scheme mechanism of Au–TiO2/WO3 for H2 production; (c–e) Schematic illustration of the mechanism for photocatalytic water splitting in core-shell NiS/TiO2 heterojunction.[76,78]

G is a one atom thick 2D material of an indefinite number of sp^2-hybridized carbon atoms in hexagonal arrangement. The thickness of isolated G sheets is 0.34 nm, accordingly, G is the physical limit in the miniaturization of a 2D material. G is the structural constitutive unit of graphite, which is obtained by strictly ordered stacking in the vertical direction of G layers. The crystal structure of graphite and the stacking derives from the strong ð-ð interactions between the G layers. G and G-based materials have attracted considerable interest in recent years due to their unique mechanical, physical and chemical properties [90]. In contrast to graphite, G is extremely robust, flexible and elastic, having a Young's modulus several orders of magnitude higher than steel. Although G has been considered a "flat surface", G layers can bent showing wrinkles and a more corrugated morphology (see Figure 9 (a,b)). The extended ð orbital of G has electron density above and below the basal plane. This extended conjugation is responsible for the high-electrical and thermal conductivity of G as well as the high adsorption capacity and the strong interaction with transition metals as commented later. Moreover, G morphology provides a large specific surface area. Theoretical calculations estimate that single layer G should have a specific surface area of approximately 2650 m^2/g, which is largest than, for instance, most zeolites and other inorganic porous materials. As consequence of these properties G is considered as a material having totally accessible sites on large surface area with exposed ð orbitals free to interact with substrates. All these features are very convenient for catalytic applications. In fig. 10, it shows hydrogen evolution amount. Based on the above results, 0.32 M formic acid and 0.013 g L^{-1} photocatalyst were chosen to conduct the photocatalytic water splitting experiments. The photocatalytic H_2 production efficiencies of MoS_2/graphene hybrid materials with different amounts of graphene[91]. It can be seen that MSG0.8 photocatalyst could achieve the maximum hydrogen evolution rate at 667.2 ìmol g^{-1} h^{-1}.

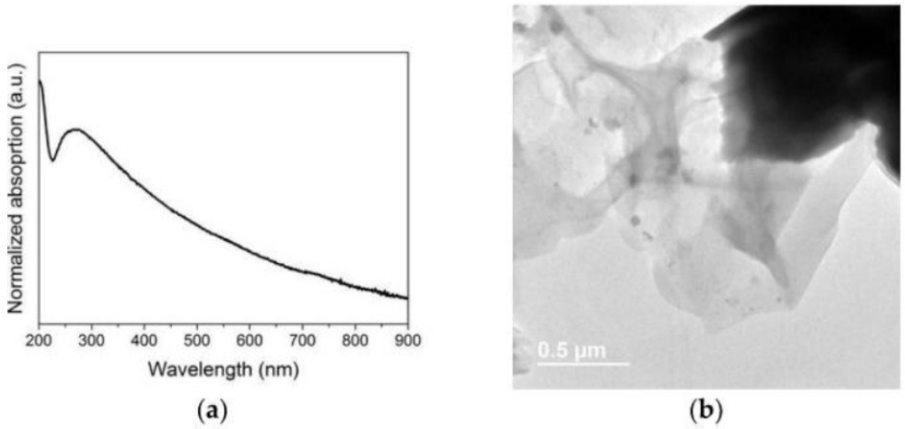

Fig. 9. (a) Absorption spectrum of a few layers defective G film obtained from the pyrolysis of alginic acid. (b) HRTEM image of a G sheet characterized by a very light contrast.[90]

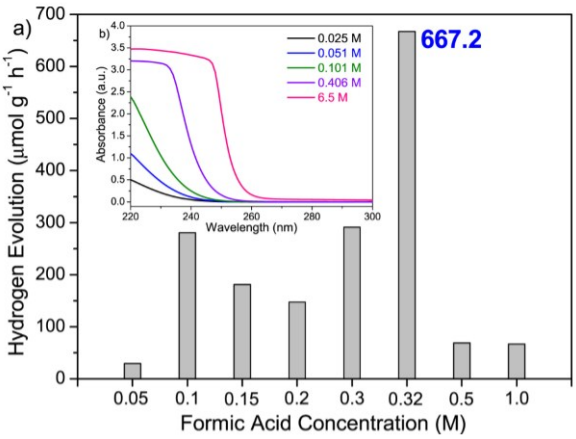

Fig. 10. Photocatalytic Hydrogen evolution via water splitting.[91]

4. Conclusion

In conclusion, regardless of the previous reports, the probability of TiO_2 and g-C_3N_4 modification for more efficient photocatalytic water splitting apparently has not been fully discovered. While the challenges in heterojunction have not been studied in detail, Z-scheme photocatalytic system is like the natural photosynthesis. It is recommended that full exploration of this can results in discovery in the efficiency of photocatalytic activity while using monolith photoreactor system. As a concluding remark, both opportunities and challenges are present in future development of this encouraging technology. Ideally, this review will enhance further advancement of TiO_2 and g-C_3N_4 modification for attaining its application for effective photocatalytic water splitting in the presence of sacrificial reagents with different types of photo reactors. Z-scheme coupling mechanism enables a wider band gap semiconductor photocatalyst to achieve stronger redox potential, while simultaneously makes it active for absorption of visible light. Doping increases the charge separation and improves the range of photoexcitation. Recently, there is very little knowledge about the monolith photoreactor for photocatalytic water splitting. The monolith photoreactor, in which reaction is conducted in a gas phase, can lead to a new development in the reactor design due to higher photon flux utilization with larger illuminated surface area. It can inhibit the side product during the production of H_2 due to efficient absorption process, surface reactions and minimum mass transfer limitations. Hence, the monolith photo reactor can be expected to produce more yield of H_2 with higher selectivity. It is well known that operating parameters such as temperature and pH also can enhance the efficiency of the photocatalysts. In addition, narrowing the band gap and controlling catalyst morphology enables efficient H2 production. Therefore, future researches in catalyst synthesis Structural modifications lead to larger surface area, provides more active site and higher visible light absorption for maximizing photocatalytic activity, and surface modification is necessary for the purpose of tuning the band gap to enhance visible light absorption with minimum charges recombination.

References

[1] Ahmad, H., Kamarudin, S.K., Minggu, L.J. and Kassim, M., 2015. Hydrogen from photo-catalytic water splitting process: A review. Renewable and Sustainable Energy Reviews, 43, pp.599-610.

[2] Gupta, N.M., 2017. Factors affecting the efficiency of a water splitting photocatalyst: a perspective. Renewable and Sustainable Energy Reviews, 71, pp.585-601.

[3] Dubey, P.K., Tripathi, P., Tiwari, R.S., Sinha, A.S.K. and Srivastava, O.N., 2014. Synthesis of reduced graphene oxide–TiO2 nanoparticle composite systems and its application in hydrogen production. international journal of hydrogen energy, 39(29), pp.16282-16292.

[4] Tee, S.Y., Win, K.Y., Teo, W.S., Koh, L.D., Liu, S., Teng, C.P. and Han, M.Y., 2017. Recent progress in energy driven water splitting. Advanced science, 4(5), p.1600337.

[5] Acar, C. and Dincer, I., 2015. Impact assessment and efficiency evaluation of hydrogen production methods. International journal of energy research, 39(13), pp.1757-1768.

[6] Zhu, J. and Zäch, M., 2009. Nanostructured materials for photocatalytic hydrogen production. Current Opinion in Colloid & Interface Science, 4(14), pp.260-269.

[7] Muradov, N.Z. and Veziroðlu, T.N., 2008. "Green" path from fossil-based to hydrogen economy: an overview of carbon-neutral technologies. International journal of hydrogen energy, 33(23), pp.6804-6839.

[8] Fujishima, A. and Honda, K., 1972. Electrochemical photolysis of water at a semiconductor electrode. nature, 238(5358), pp.37-38.

[9] Fajrina, N. and Tahir, M., 2019. A critical review in strategies to improve photocatalytic water splitting towards hydrogen production. International Journal of Hydrogen Energy, 44(2), pp.540-577.

[10] Lin, Y., Jiang, Z., Zhu, C., Hu, X., Zhu, H., Zhang, X., Fan, J. and Lin, S.H., 2013. The optical absorption and hydrogen production by water splitting of (Si, Fe)-codoped anatase TiO2 photocatalyst. International journal of hydrogen energy, 38(13), pp.5209-5214.

[11] Ye, S., Wang, R., Wu, M.Z. and Yuan, Y.P., 2015. A review on g-C3N4 for photocatalytic water splitting and CO2 reduction. Applied Surface Science, 358, pp.15-27.

[12] Li, H., Tu, W., Zhou, Y. and Zou, Z., 2016. Z Scheme photocatalytic systems for promoting photocatalytic performance: recent progress and future challenges. Advanced Science, 3(11), p.1500389.

[13] Boudjemaa, A., Rebahi, A., Terfassa, B., Chebout, R., Mokrani, T., Bachari, K. and Coville, N.J., 2015. Fe2O3/carbon spheres for efficient photo-catalytic hydrogen production from water and under visible light irradiation. Solar Energy Materials and Solar Cells, 140, pp.405-411.

[14] Ling, C., Xue, Q., Han, Z., Zhang, Z., Du, Y., Liu, Y. and Yan, Z., 2014. High hydrogen response of Pd/TiO2/SiO2/Si multilayers at room temperature. Sensors and Actuators B: Chemical, 205, pp.255-260.

[15] Xu, Y. and Xu, R., 2015. Nickel-based cocatalysts for photocatalytic hydrogen production. Applied Surface Science, 351, pp.779-793.

[16] Wen, J., Xie, J., Chen, X. and Li, X., 2017. A review on g-C3N4-based photocatalysts. Applied surface science, 391, pp.72-123.

[17] Zhu, J. and Zäch, M., 2009. Nanostructured materials for photocatalytic hydrogen production. Current Opinion in Colloid & Interface Science, 4(14), pp.260-269.

[18] Acar, C., Dincer, I. and Zamfirescu, C., 2014. A review on selected heterogeneous photocatalysts for hydrogen production. International Journal of Energy Research, 38(15), pp.1903-1920.

[19] Sarathy, V., Tratnyek, P.G., Nurmi, J.T., Baer, D.R., Amonette, J.E., Chun, C.L., Penn, R.L. and Reardon, E.J., 2008. Aging of iron nanoparticles in aqueous solution: effects on structure and reactivity. The Journal of Physical Chemistry C, 112(7), pp.2286-2293.

[20] Zhang, Y., Xu, J.L., Xu, H.J., Yuan, Z.H. and Guo, Y., 2010. Cellulase deactivation based kinetic modeling of enzymatic hydrolysis of steam-exploded wheat straw. Bioresource technology, 101(21), pp.8261-

8266.

[21] Theron, J., Walker, J.A. and Cloete, T.E., 2008. Nanotechnology and water treatment: applications and emerging opportunities. Critical reviews in microbiology, 34(1), pp.43-69.

[22] Hwang, Y.H., Kim, D.G., Ahn, Y.T., Moon, C.M. and Shin, H.S., 2010. Fate of nitrogen species in nitrate reduction by nanoscale zero valent iron and characterization of the reaction kinetics. Water Science and Technology, 61(3), pp.705-712.

[23] Todaka, Y., Tsuchiya, K., Umemoto, M., Sasaki, M. and Imai, D., 2003. Growth of Fe3O4 whiskers from solid solution nanoparticles of Fe–Cu and Fe–Ag systems produced by DC plasma jet method. Materials Science and Engineering: A, 340(1-2), pp.114-122.

[24] Nurmi, J.T., Tratnyek, P.G., Sarathy, V., Baer, D.R., Amonette, J.E., Pecher, K., Wang, C., Linehan, J.C., Matson, D.W., Penn, R.L. and Driessen, M.D., 2005. Characterization and properties of metallic iron nanoparticles: spectroscopy, electrochemistry, and kinetics. Environmental science & technology, 39(5), pp.1221-1230.

[25] Phenrat, T., Saleh, N., Sirk, K., Tilton, R.D. and Lowry, G.V., 2007. Aggregation and sedimentation of aqueous nanoscale zerovalent iron dispersions. Environmental Science & Technology, 41(1), pp.284-290.

[26] Wang, C.B. and Zhang, W.X., 1997. Synthesizing nanoscale iron particles for rapid and complete dechlorination of TCE and PCBs. Environmental science & technology, 31(7), pp.2154-2156.

[27] Zhang, L. and Manthiram, A., 1997. Chains composed of nanosize metal particles and identifying the factors driving their formation. Applied physics letters, 70(18), pp.2469-2471.

[28] Baret, G., 2014. Use of Nanomaterials in Water Remediation by a Subcritical Water Process. Aquananotechnology: Global Prospects, p.55.

[29] Sun, Y.P., Li, X.Q., Cao, J., Zhang, W.X. and Wang, H.P., 2006. Characterization of zero-valent iron nanoparticles. Advances in colloid and interface science, 120(1-3), pp.47-56.

[30] Štengl, V. and Králová, D., 2011. TiO2/ZnS/CdS nanocomposite for hydrogen evolution and orange II dye degradation. International Journal of Photoenergy, 2011.

[31] An, L., Han, X., Li, Y., Hou, C., Wang, H. and Zhang, Q., 2019. ZnS–CdS–TaON nanocomposites with enhanced stability and photocatalytic hydrogen evolution activity. Journal of Sol-Gel Science and Technology, 91(1), pp.82-91.

[32] Biswas, M.R.U.D., Ali, A., Cho, K.Y. and Oh, W.C., 2018. Novel synthesis of WSe2-Graphene-TiO2 ternary nanocomposite via ultrasonic technics for high photocatalytic reduction of CO2 into CH3OH. Ultrasonics sonochemistry, 42, pp.738-746.

[33] Biswas, M.R.U.D., Ali, A., Cho, K.Y. and Oh, W.C., 2018. Novel synthesis of WSe2-Graphene-TiO2 ternary nanocomposite via ultrasonic technics for high photocatalytic reduction of CO2 into CH3OH. Ultrasonics sonochemistry, 42, pp.738-746.

[34] Ha Huu Do, Dang Le Tri Nguyen, Xuan Cuong Nguyen, Thu-Ha Le, Thang Phan Nguyen, Quang Thang Trinh, Sang Hyun Ahn, Dai-Viet N. Vo, Soo Young Kim, Quyet Van Le ,mVolume 13, Issue 2, February 2020, Pages 3653-3671.

[35] J. Meng, Q. Lin, T. Chen, X. Wei, J. Li, Z. Zhang, Oxygen vacancy regulation on tungsten oxides with specific exposed facets for enhanced visible-light-driven photocatalytic oxidation, Nanoscale (2018) 2908-2915.

[36] G. Zhang, W. Zhang, J. Crittenden, D. Minakata, Y. Chen, P. Wang, Effects of inorganic electron donors in photocatalytic hydrogen production over Ru/ (CuAg)0.15In0.3Zn1.4S2 under visible light irradiation, J. Renew. Sustain. Energy 6 (2014) 09, https://doi.org/10.1063/1.4884197.

[37] H. Liu, J. Yuan, W. Shangguan, Photochemical reduction and oxidation of water including sacrificial reagents and Pt/TiO2 catalyst, Energy Fuels 20 (2006) 2289-2292, https://doi.org/10.1021/ef060174n.

[38] Ashok kumar, M., 1998. An overview on semiconductor particulate systems for photoproduction of hydrogen. International Journal of Hydrogen Energy, 23(6), pp.427-438.

[39] Zou, Z., Ye, J., Sayama, K. and Arakawa, H., 2001. Direct splitting of water under visible light irradiation with an oxide semiconductor photocatalyst. nature, 414(6864), pp.625-627.

[40] Li, Q. and Lu, G., 2007. Visible-light driven photocatalytic hydrogen generation on Eosin Y-sensitized Pt-loaded nanotube Na2Ti2O4 (OH) 2. Journal of Molecular Catalysis A: Chemical, 266(1-2), pp.75-79.

[41] Lettmann, C., Hinrichs, H. and Maier, W.F., 2001. Combinatorial discovery of new photocatalysts for water purification with visible light. Angewandte Chemie International Edition, 40(17), pp.3160-3164.

[42] Jaramillo, T.F., Baeck, S.H., Kleiman-Shwarsctein, A., Choi, K.S., Stucky, G.D. and McFarland, E.W., 2005. Automated Electrochemical Synthesis and Photoelectrochemical Characterization of Zn1-x Co x O Thin Films for Solar Hydrogen Production. Journal of combinatorial chemistry, 7(2), pp.264-271.

[43] Kudo, A., 2006. Development of photocatalyst materials for water splitting. International Journal of Hydrogen Energy, 31(2), pp.197-202.

[44] Liu, H., Yuan, J. and Shangguan, W., 2006. Photochemical reduction and oxidation of water including sacrificial reagents and Pt/TiO2 catalyst. Energy & fuels, 20(6), pp.2289-2292.

[45] Maeda, K., Teramura, K. and Domen, K., 2008. Effect of post-calcination on photocatalytic activity of (Ga1" xZnx)(N1" xOx) solid solution for overall water splitting under visible light. Journal of catalysis, 254(2), pp.198-204.

[46] Tsuji, I., Kato, H., Kobayashi, H. and Kudo, A., 2004. Photocatalytic H2 evolution reaction from aqueous solutions over band structure-controlled (AgIn) x Zn2 (1-x) S2 solid solution photocatalysts with visible-light response and their surface nanostructures. Journal of the American Chemical Society, 126(41), pp.13406-13413.

[47] Yao, W. and Ye, J., 2006. Photophysical and Photocatalytic Properties of Ca1-x Bi x V x Mo1-x O4 Solid Solutions. The Journal of Physical Chemistry B, 110(23), pp.11188-11195.

[48] Li, Y., Chen, G., Zhou, C. and Sun, J., 2009. A simple template-free synthesis of nanoporous ZnS–In2S3–Ag2S solid solutions for highly efficient photocatalytic H2 evolution under visible light. Chemical communications, (15), pp.2020-2022.

[49] Xing, C., Zhang, Y., Yan, W. and Guo, L., 2006. Band structure-controlled solid solution of Cd1-x ZnxS photocatalyst for hydrogen production by water splitting. International Journal of Hydrogen Energy, 31(14), pp.2018-2024.

[50] Zhang, K., Jing, D., Xing, C. and Guo, L., 2007. Significantly improved photocatalytic hydrogen production activity over Cd1-xZnxS photocatalysts prepared by a novel thermal sulfuration method. International Journal of Hydrogen Energy, 32(18), pp.4685-4691.

[51] Yang, H., Guo, L., Yan, W. and Liu, H., 2006. A novel composite photocatalyst for water splitting hydrogen production. Journal of Power Sources, 159(2), pp.1305-1309.

[52] Liu, Y., Guo, L., Yan, W. and Liu, H., 2006. A composite visible-light photocatalyst for hydrogen production. Journal of power Sources, 159(2), pp.1300-1304.

[53] Jing, D. and Guo, L., 2007. Hydrogen production over Fe-doped tantalum oxide from an aqueous methanol solution under the light irradiation. Journal of Physics and Chemistry of Solids, 68(12), pp.2363-2369.

[54] Shen, S. and Guo, L., 2006. Structural, textural and photocatalytic properties of quantum-sized In2S3-sensitized Ti-MCM-41 prepared by ion-exchange and sulfidation methods. Journal of Solid State Chemistry, 179(8), pp.2629-2635.

[55] Shen, S. and Guo, L., 2008. Growth of quantum-confined CdS nanoparticles inside Ti-MCM-41 as a visible light photocatalyst. Materials Research Bulletin, 43(2), pp.437-446.

[56] Xing, C., Jing, D., Liu, M. and Guo, L., 2009. Photocatalytic hydrogen production over Na2Ti2O4 (OH) 2 nanotube sensitized by CdS nanoparticles. Materials Research Bulletin, 44(2), pp.442-445.

[57] Shehzad, N., Tahir, M., Johari, K., Murugesan, T. and Hussain, M., 2018. A critical review on TiO2

based photocatalytic CO2 reduction system: Strategies to improve efficiency. Journal of CO2 Utilization, 26, pp.98-122.

[58] Coll, M., Fontcuberta, J., Althammer, M., Bibes, M., Boschker, H., Calleja, A., Cheng, G., Cuoco, M., Dittmann, R., Dkhil, B. and El Baggari, I., 2019. Towards oxide electronics: a roadmap. Applied surface science, 482, pp.1-93.

[59] Wang, Z., Guan, W., Sun, Y., Dong, F., Zhou, Y. and Ho, W.K., 2015. Water-assisted production of honeycomb-like gC 3 N 4 with ultralong carrier lifetime and outstanding photocatalytic activity. Nanoscale, 7(6), pp.2471-2479.

[60] Bai, X., Wang, L., Zong, R. and Zhu, Y., 2013. Photocatalytic activity enhanced via g-C3N4 nanoplates to nanorods. The Journal of Physical Chemistry C, 117(19), pp.9952-9961.

[61] Chen, Y., Wang, B., Lin, S., Zhang, Y. and Wang, X., 2014. Activation of n'! À* transitions in two-dimensional conjugated polymers for visible light photocatalysis. The Journal of Physical Chemistry C, 118(51), pp.29981-29989.

[62] Zheng, D., Pang, C., Liu, Y. and Wang, X., 2015. Shell-engineering of hollow gC 3 N 4 nanospheres via copolymerization for photocatalytic hydrogen evolution. Chemical Communications, 51(47), pp.9706-9709.

[63] Zhang, J., Huang, Y., Nie, T., Wang, R., He, B., Han, B., Wang, H., Tian, Y. and Gong, Y., 2020. Enhanced visible-light photocatalytic H2 production of hierarchical g-C3N4 hexagon by one-step self-assembly strategy. Applied Surface Science, 499, p.143942.

[64] Chen, Z., Yang, S., Tian, Z. and Zhu, B., 2019. NiS and graphene as dual cocatalysts for the enhanced photocatalytic H2 production activity of g-C3N4. Applied Surface Science, 469, pp.657-665.

[65] Xu, Y., Li, Y., Wang, P., Wang, X. and Yu, H., 2018. Highly efficient dual cocatalyst-modified TiO2 photocatalyst: RGO as electron-transfer mediator and MoSx as H2-evolution active site. Applied Surface Science, 430, pp.176-183.

[66] Azam, M.U., Tahir, M., Umer, M., Tahir, B., Shehzad, N. and Siraj, M., 2019. In-situ synthesis of TiO2/La2O2CO3/rGO composite under acidic/basic treatment with La3+/Ti3+ as mediators for boosting photocatalytic H2 evolution. International Journal of Hydrogen Energy, 44(42), pp.23669-23688.

[67] Wen, J., Li, X., Li, H., Ma, S., He, K., Xu, Y., Fang, Y., Liu, W. and Gao, Q., 2015. Enhanced visible-light H2 evolution of g-C3N4 photocatalysts via the synergetic effect of amorphous NiS and cheap metal-free carbon black nanoparticles as co-catalysts. Applied Surface Science, 358, pp.204-212.

[68] Zhang, W., Wang, Y., Wang, Z., Zhong, Z. and Xu, R., 2010. Highly efficient and noble metal-free NiS/CdS photocatalysts for H 2 evolution from lactic acid sacrificial solution under visible light. Chemical Communications, 46(40), pp.7631-7633.

[69] Ji, C., Yin, S.N., Sun, S. and Yang, S., 2018. An in situ mediator-free route to fabricate Cu2O/g-C3N4 type-II heterojunctions for enhanced visible-light photocatalytic H2 generation. Applied Surface Science, 434, pp.1224-1231.

[70] He, K., Xie, J., Li, M. and Li, X., 2018. In situ one-pot fabrication of g-C3N4 nanosheets/NiS cocatalyst heterojunction with intimate interfaces for efficient visible light photocatalytic H2 generation. Applied Surface Science, 430, pp.208-217.

[71] Jia, J., Sun, W., Zhang, Q., Zhang, X., Hu, X., Liu, E. and Fan, J., 2020. Inter-plane heterojunctions within 2D/2D FeSe2/g-C3N4 nanosheet semiconductors for photocatalytic hydrogen generation. Applied Catalysis B: Environmental, 261, p.118249.

[72] Chang, D.W. and Baek, J.B., 2016. Nitrogen Doped Graphene for Photocatalytic Hydrogen Generation. Chemistry–An Asian Journal, 11(8), pp.1125-1137.

[73] Jeon, I.Y., Choi, H.J., Jung, S.M., Seo, J.M., Kim, M.J., Dai, L. and Baek, J.B., 2013. Large-scale production of edge-selectively functionalized graphene nanoplatelets via ball milling and their use as metal-free electrocatalysts for oxygen reduction reaction. Journal of the American Chemical Society, 135(4), pp.1386-1393.

[74] Mou, Z., Wu, Y., Sun, J., Yang, P., Du, Y. and Lu, C., 2014. TiO2 nanoparticles-functionalized N-doped graphene with superior interfacial contact and enhanced charge separation for photocatalytic hydrogen generation. ACS Applied Materials & Interfaces, 6(16), pp.13798-13806.

[75] Fajrina, N. and Tahir, M., 2020. Monolithic Ag-Mt dispersed Z-scheme pCN-TiO2 heterojunction for dynamic photocatalytic H2 evolution using liquid and gas phase photoreactors. International Journal of Hydrogen Energy, 45(7), pp.4355-4375.

[76] Mohamed, R.M., Kadi, M.W. and Ismail, A.A., 2020. A Facile synthesis of mesoporous á-Fe2O3/TiO2 nanocomposites for hydrogen evolution under visible light. Ceramics International.

[77] Zhao, X., Xie, W., Deng, Z., Wang, G., Cao, A., Chen, H., Yang, B., Wang, Z., Su, X. and Yang, C., 2020. Salt templated synthesis of NiO/TiO2 supported carbon nanosheets for photocatalytic hydrogen production. Colloids and Surfaces A: Physicochemical and Engineering Aspects, 587, p.124365.

[78] Jia, J., Wang, Q. and Wang, Y., 2019. Synthesis of BixTiyOz/TiO2 heterojunction with enhanced visible-light photocatalytic activity and mechanism insight. Journal of Alloys and Compounds, 809, p.151791.

[79] Tiwari, A. and Pal, U., 2015. Effect of donor-donor- p-acceptor architecture of triphenylamine-based organic sensitizers over TiO2 photocatalysts for visiblelight-driven hydrogen production. international journal of hydrogen energy, 40(9069), p.e9079..

[80] Humayun, M., Zada, A., Li, Z., Xie, M., Zhang, X., Qu, Y., Raziq, F. and Jing, L., 2016. Enhanced visible-light activities of porous BiFeO3 by coupling with nanocrystalline TiO2 and mechanism. Applied Catalysis B: Environmental, 180, pp.219-226.

[81] Umer, M., Tahir, M., Azam, M.U., Tahir, B., Jaffar, M.M. and Alias, H., 2019. Montmorillonite dispersed single wall carbon nanotubes (SWCNTs)/TiO2 heterojunction composite for enhanced dynamic photocatalytic H2 production under visible light. Applied Clay Science, 174, pp.110-119.

[82] Lucci, F., Della Torre, A., Montenegro, G. and Eggenschwiler, P.D., 2015. On the catalytic performance of open cell structures versus honeycombs. Chemical Engineering Journal, 264, pp.514-521.

[83] Meng, A., Zhu, B., Zhong, B., Zhang, L. and Cheng, B., 2017. Direct Z-scheme TiO2/CdS hierarchical photocatalyst for enhanced photocatalytic H2-production activity. Applied Surface Science, 422, pp.518-527.

[84] Zhang, D., Ma, X., Zhang, H., Liao, Y. and Xiang, Q., 2018. Enhanced photocatalytic hydrogen evolution activity of carbon and nitrogen self-doped TiO2 hollow sphere with the creation of oxygen vacancy and Ti3+. Materials today energy, 10, pp.132-140.

[85] Gong, H., Liu, Q. and Huang, C., 2019. NiSe as an effective co-catalyst coupled with TiO2 for enhanced photocatalytic hydrogen evolution. International Journal of Hydrogen Energy, 44(10), pp.4821-4831.

[86] Linsebigler, A.L., Lu, G. and Yates Jr, J.T., 1995. Photocatalysis on TiO2 surfaces: principles, mechanisms, and selected results. Chemical reviews, 95(3), pp.735-758.

[87] Kumaravel, V., Mathew, S., Bartlett, J. and Pillai, S.C., 2019. Photocatalytic hydrogen production using metal doped TiO2: A review of recent advances. Applied Catalysis B: Environmental, 244, pp.1021-1064.

[88] Lv, Y.R., Liu, C.J., He, R.K., Li, X. and Xu, Y.H., 2019. BiVO4/TiO2 heterojunction with enhanced photocatalytic activities and photoelectochemistry performances under visible light illumination. Materials Research Bulletin, 117, pp.35-40.

[89] Tahir, M., Siraj, M., Tahir, B., Umer, M., Alias, H. and Othman, N., 2020. Au-NPs embedded Z–scheme WO3/TiO2 nanocomposite for plasmon-assisted photocatalytic glycerol-water reforming towards enhanced H2 evolution. Applied Surface Science, 503, p.144344.

[90] Robertson, A.W., Bachmatiuk, A., Wu, Y.A., Schaffel, F., Rellinghaus, B., Buchner, B., Rummeli, M.H. and Warner, J.H., 2011. Atomic structure of interconnected few-layer graphene domains. ACS nano, 5(8), pp.6610-6618.

[91] Albero, J., Mateo, D. and García, H., 2019. Graphene-based materials as efficient photocatalysts for water splitting. Molecules, 24(5), p.906.